Another significant implication of earthquake induced-period lengthening is that the latter is a key parameter in the ground motion selection and scaling procedure, as most current seismic codes define the spectral matching period bandwidth on the basis of the fundamental period of structures. This is of particular interest for Eurocode 8 [19], which, in contrast to the US codes and guidelines such as ASCE/SEI 7-10 [20] and FEMA P-750 [21], enforces a wider spectral matching period range that extends up to twice the fundamental period of the building (as opposed to 1.5 times prescribed in the US). This difference may potentially result in overconservative and highly scattered estimates of seismic demand for reasons described elsewhere [22].

To investigate further the extent of period elongation during strong ground motion and its implications in the design and assessment of structures, a group of five R/C buildings [23] with various structural configurations and dynamic characteristics was thoroughly studied. The buildings, designed deliberately for various ductility classes according to modern seismic codes (herein Eurocode 8), were transformed into equivalent nonlinear single-degree-of-freedom (SDOF) systems [24] of various hysteretic rules and then they were subjected to a set of carefully selected ground motions. In the following, the correlation patterns observed between the numerically predicted periods lengthening of the five buildings studied, the structural properties and the ground motion characteristics are presented and critically assessed.

2. Strong ground motion selection

In contrast to the common practice where ground motion selection is either based on a given, site-specific seismic hazard scenario, or involves a small number of recorded ground motions (which typically does not exceed seven), the scope of the particular investigation dictated the formation of a large ensemble of earthquake records with a wealth of different characteristics. For this purpose, an ensemble of 300 seismic motions was formed according to particular selection rules to prevent undesirable bias. More precisely:

(a) Forty-three (43) different earthquake events recorded in various regions worldwide were employed to avoid dominating the ensemble with records from areas with common seismotectonic features.
(b) The maximum number of records from the same earthquake event was limited to less than 15% of the total, while only one of the two horizontal components was used from the same station.
(c) The preliminary selection criteria related to seismological characteristics (i.e., magnitude, rupture mechanism, directivity of seismic waves), amplitude (peak ground acceleration) and soil profile were deliberately kept wide.
(d) Both near-and far-field seismic motions were used to provide high amplifications in a wide range of structural periods. Given that the aim of the study is to investigate the predominant inelastic period under strong ground motion, short duration motions were filtered-out (i.e., a $M_w > 5.5$ criterion was adopted), as weaker motions would statistically lead to lower ductility demand. Fig. 1 illustrates the distribution of the selected strong motion characteristics in terms of earthquake magnitude, source-to-site distance, and peak ground acceleration (PGA).
(e) The mean period parameter (T_m) was introduced, to quantify the predominant frequency content of the records used [25], as a means to retain the ensemble as uniformly distributed as possible. Different intervals of T_m, indicative of high, moderate and low-frequency content, were defined (Table 1) and three frequency-based subsets of 100 records were formed, each characterized by high spectral amplifications in the short, moderate and long period range respectively. It is recalled that the mean period, T_m, is derived by weighting the amplitudes over a specified range of the Fourier Amplitude Spectrum (FAS):

$$T_m = \frac{\sum C_i^2 \frac{1}{f_i}}{\sum C_i^2} \quad \text{for } 0.25\ \text{Hz} \leqslant f_i \leqslant 20\ \text{Hz with } \Delta f \leqslant 0.05\ \text{Hz} \tag{1}$$

where C_i are the Fourier amplitude coefficients, f_i are the discrete Fast Fourier Transformation (FFT) frequencies between 0.25 and 20 Hz and Δf is the frequency interval used in the FFT.

Based on the above criteria, the ground motions summarized in Table 2 were retrieved by the PEER-NGA Database [26] and were later applied for the excitation of the five R/C buildings presented in the following section.

3. Structural models

3.1. Multiple degree of freedom systems

The structures selected for this investigation have been extensively studied in the past [23,27,28] and represent alternative and realistic structural configurations in terms of the earthquake resistant system (frame or dual), their ductility level (Classes High and Low according to the Eurocode 8) and their overall height (and subsequently, their fundamental period). Live loads and permanent gravity load are both assumed equal to 2.0 kN/m^2. All buildings are assumed to be supported on (firm) soil class 'B' according to EC8. The characteristic cylinder strength of concrete was taken 30 N/mm^2 and the yield strength of steel equal to 585 N/mm^2 for both longitudinal and transverse reinforcement. More details regarding member cross section sizes and reinforcements are given in [27].

It is noted that the intention was to examine buildings designed to modern seismic codes in order to focus on a better-controlled stock with identical level of seismic safety. On the other hand, it is evident that existing, pre-code, or under-designed structures

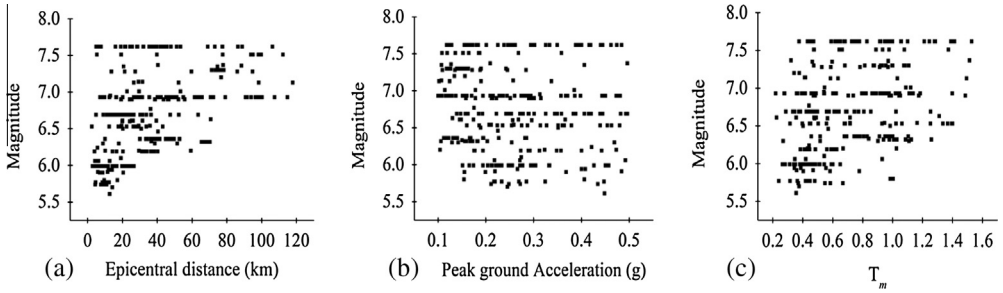

Fig. 1. Distribution of the selected strong motion characteristics in terms of earthquake magnitude, source-to-site distance, peak ground acceleration and mean period.

Table 1
Distribution of selected earthquake ground motions in terms of their mean period T_m.

Subset number	T_m interval (s)	Number of records	25th Percentile (Q1) of T_m (s)	50th Percentile (Q2) of T_m (s)	75th Percentile (Q3) of T_m (s)
1	0.10–0.50	100	0.30	0.37	0.44
2	0.50–0.90	100	0.58	0.66	0.78
3	0.90–1.55	100	0.99	1.08	1.19

Table 2
Earthquake events used in the study and related information (retrieved from PEER-NGA Database, Chiou et al. [26]).

Earthquake name (date)	Magnitude, M_w	Number of records	Distance (km) R_{min}–R_{max}	Site class[a,b]
Kern County (1952.07.21)	7.36	1	88.39	C(1)
North. California (1954.12.21)	6.50	1	30.79	D(1)
Parkfield (1966.06.28)	6.19	3	32.56–40.26	C(1) + D(2)
Borrego Mountain (1968.04.09)	6.63	1	70.75	D(1)
San Fernando (1971.02.09)	6.61	5	20.04–39.49	C(4) + D(1)
Managua, Nicaragua (1972.12.23)	6.24	1	5.68	D(1)
Friuli, Italy (1976.05.06)	6.50	1	20.23	C(1)
Tabas, Iran (1978.09.16)	7.35	2	20.63–74.66	C(1) + D(1)
Coyote Lake (1979.08.06)	5.74	4	4.37–10.94	C(1) + D(3)
Imperial Valley (1979.10.15)	6.53	18	2.47–43.15	D(18)
Livermore (1980.01.24)	5.80	1	17.13	D(1)
Mammoth Lakes (1980.05.25)	5.94	7	5.90–14.19	D(7)
Victoria, Mexico (1980.06.09)	6.33	1	36.67	D(1)
Trinidad and Tobago (1980.11.08)	7.20	2	76.75	D(2)
Corinth, Greece (1981.02.24)	6.60	1	19.92	D(1)
Westmorland (1981.04.26)	5.90	3	7.02–20.47	D(3)
Coalinga (1983.05.02)	6.36	22	4.60–52.86	C(9) + D(13)
Morgan Hill (1984.04.24)	6.19	5	3.94–38.20	C(2) + D(3)
Taiwan-SMART1-40 (1986.05.20)	6.32	8	65.48–70.27	D(8)
N.Palm Springs (1986.07.08)	6.06	2	4.24–6.28	D(2)
Chalfant Valley (1986.07.20)	6.19	4	10.54–31.25	D(4)
San Salvador, El Salv. (1986.10.10)	5.80	1	9.54	D(1)
Taiwan-SMART1-45 (1986.11.14)	7.30	15	71.35–78.21	C(1) + D(14)
New Zealand (1987.03.02)	6.60	1	24.23	C(1)
Whittier Narrows (1987.10.01)	5.99	25	2.86–26.55	C(11) + D(14)
Superstition Hills (1987.11.24)	6.54	3	19.51–35.83	D(3)
Spitak, Armenia (1988.12.07)	6.77	1	36.19	D(1)
Loma Prieta (1989.10.18)	6.93	42	7.17–114.87	B(1) + C(19) + D(17) + E(5)
Manjil, Iran (1990.06.20)	7.37	2	40.43–77.84	C(1) + D(1)
Sierra Madre (1991.06.28)	5.61	1	12.64	C(1)
Erzincan, Turkey (1992.03.13)	6.69	1	8.97	D(1)
Cape Mendocino (1992.04.25)	7.01	3	22.64–53.34	C(1) + D(2)
Landers (1992.06.28)	7.28	6	13.67–94.77	C(2) + D(4)
Big Bear (1992.06.28)	6.46	1	40.46	D(1)
Northridge (1994.01.17)	6.69	33	4.85–63.53	A(1) + B(1) + C(16) + D(15)
Kobe, Japan (1995.01.16)	6.90	10	19.25–55.81	A(1) + D(9)
Northwest China (1997.04.11)	6.10	1	19.11	D(1)
Kocaeli, Turkey (1999.08.17)	7.51	9	5.31–112.26	B(1) + C(1) + D(6) + E(1)
Chi-Chi, Taiwan-1 (1999.09.20)	7.62	39	4.96–106.20	C(31) + D(8)
Chi-Chi, Taiwan-2 (1999.09.20)	6.20	3	10.10–59.29	C(2) + D(1)
Chi-Chi, Taiwan-3 (1999.09.25)	6.30	4	8.80–51.51	C(2) + D(2)
Hector Mine (1999.10.16)	7.13	4	26.53–117.88	C(2) + D(2)
Duzce, Turkey (1999.11.12)	7.14	2	29.27–31.56	C(1) + D(1)

[a] According to the NEHRP site classification: Site class A ($v_{s,30} \geqslant 1500$ m/s), Site class B (760 m/s < $v_{s,30} \leqslant 1500$ m/s), Site class C (360 m/s < $v_{s,30} \leqslant 760$ m/s), Site class D (180 m/s < $v_{s,30} \leqslant 360$ m/s) and Site class E ($v_{s,30} \leqslant 180$).
[b] In the last column, number in the parenthesis indicates the number of records for given site class.

with low yield strength are expected to be more prone to inelastic deformations and thus, to period lengthening or vulnerable to premature failure due to inadequate shear strength. For this reason, the results of this study, strictly speaking, only apply to buildings designed to modern seismic codes.

The five buildings studied herein are illustrated in Fig. 2 and can be classified into three principal categories: regular 12-storey frames of low and high ductility (codified as 12RFDCL and 12RFDCH respectively), regular 8-storey dual systems again of low and high ductility (8SWDCL and 8SWDCH) and irregular in elevation, 8-storey frame of high ductility (8IFDCH). Particularly for the latter category, irregularity in elevation refers to the greater height and the smaller amount of columns at the base storey.

All structures examined were first modeled as two-dimensional MDOF systems using the computer code Zeus-NL [29]. Cubic 3D elastoplastic elements were used to consider the concrete behavior under cyclic loading, residual strength and stiffness degradation through a fiber approach. The non-linear model used for the concrete material is a uniaxial constant confinement concrete model (Fig. 3a), defined with the use of four parameters: compressive strength, f_c, tensile strength, f_t, crushing strain, e_{co}, and the confinement factor, k [29]. Furthermore, the reinforcement bars were modeled using a bi-linear elasto-plastic law with kinematic strain hardening, provided by Zeus-NL materials library [29]. Parameters such as the Young's modulus, E, the yield strength, f_y, and the strain-hardening parameter, n, are necessary to define this model. From the eigenvalue analysis of the five building models, the